IOP PUBLISHING NANOTECHNOLOGY
Nanotechnology **23** (2012) 205204 (5pp) doi:10.1088/0957-4484/23/20/205204

Enhanced binding strength between metal nanoclusters and carbon nanotubes with an atomic nickel defect

Dongchul Sung[1], Noejung Park[2], Gunn Kim[1] and Suklyun Hong[1,3]

[1] Department of Physics and Graphene Research Institute, Sejong University, Seoul 143-747, Korea
[2] Interdisciplinary School of Green Energy and Low Dimensional Carbon Materials Center, Ulsan National Institute of Science and Technology, 448-701, Korea

E-mail: hong@sejong.ac.kr

Received 11 January 2012, in final form 14 March 2012
Published 30 April 2012
Online at stacks.iop.org/Nano/23/205204

Abstract
Using spin-polarized density functional theory calculations, we study binding properties of small metal nanoclusters (Cu_{13} and Al_{13}) onto carbon nanotubes (CNTs). On defect-free CNTs, the binding affinity with the Cu or Al cluster is very weak. When various defects such as vacancies, substitutional nickel defects, and nickel adatoms are introduced in CNTs to increase the binding strength, the binding energies of the metal nanoclusters increase substantially irrespective of types of defects. The effect of the Ni adatom is especially noticeable. Our results propose a method for improving the wettability of metal–CNT complex composites.

(Some figures may appear in colour only in the online journal)

1. Introduction

Recently, the carbon nanotube (CNT) has been considered as a reinforcing component to enhance the mechanical properties of transition metals such as aluminum and copper [1, 2]. Reinforced light-weight composites have been required in vehicle and aircraft engineering [3–8]. For this application, it is crucial to understand the interfacial interaction between the CNT and metal. It has been considered that Cu/CNT and Al/CNT composites have substantially improved mechanical properties and maintain a good electrical conductivity. However, the binding strength between Al (or Cu) and the CNT with no defects is known to be small. Therefore, tremendous effort has been made to seek a good way to enhance binding affinity of Cu (or Al) with the CNT [4]. A previous study investigated the binding strength of metal atoms onto the defect-free and Stone–Wales (SW) defective surface of CNTs [9]. The copper and aluminum atoms are somewhat weakly bound to the CNTs (graphene) in the absence of the defect, whereas their binding strength is (slightly) increased in the presence of the SW defect. On the other hand, it was experimentally demonstrated that the mechanical strength of the CNT-incorporated copper matrix is substantially improved by introducing nickel coating layers to the CNT [3]. The purpose of this study is to understand the interaction between CNTs and the most important metals such as Al and Cu for industrial application. We focus on the effect of defects in CNTs on adsorption of metal clusters onto the CNTs. Also, we explore potential methods to increase the adhesion strength of Al or Cu metal nanoclusters onto the CNTs.

2. Calculation methods

In this study, we performed first-principles calculations using pseudopotentials and a plane-wave basis set [10] within the density functional theory (DFT) [11]. The projector augmented wave (PAW) potentials, as implemented in the Vienna *ab initio* simulation packages (VASP) [12, 13], were employed to describe the potentials from atom centers. The energy cutoff for the plane-wave basis was set to 400 eV. The generalized gradient approximation (GGA) and the localized density approximation (LDA) were used for the electrons'

[3] Author to whom any correspondence should be addressed.

Table 1. Binding energies (eV/cluster) of the metal cluster (M_{13}) on the perfect and defective (5, 5) CNTs.

Defect type	No defect		Monovacancy		Substitution		Adatom	
Metal	Cu	Al	Cu	Al	Cu	Al	Cu	Al
LDA	1.89	0.39	3.99	4.47	4.53	4.28	8.81	6.01
GGA	0.33	0.04	3.22	3.52	3.06	2.82	8.70	5.65

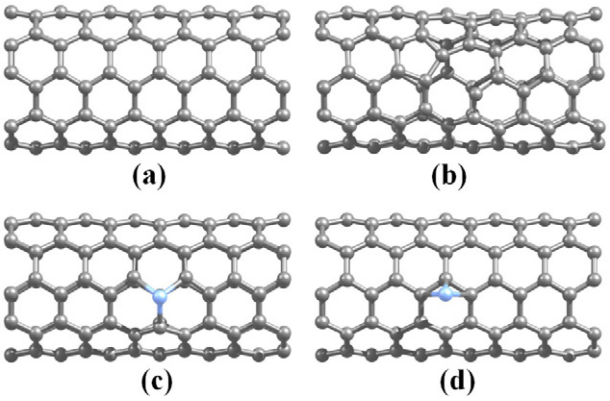

Figure 1. Optimized geometries of the (5, 5) CNTs with (a) no defect and with various defects such as (b) a monovacancy, (c) a substituted nickel atom, and (d) a nickel adatom.

exchange–correlation potential [14, 15]. Geometries were optimized until the Hellmann–Feynman forces acting on the atoms became smaller than 0.03 eV $Å^{-1}$. The (5, 5) CNT was selected as a model for CNTs. The supercell of 12 carbon layers (∼1.5 nm) was considered along the axial direction. The lateral (*xy*) dimension of the supercell (with the nanotube axis along the *z* direction) was large enough to avoid the interaction between the CNT and its images in adjacent supercells.

3. Results and discussion

We first consider defect structures on the (5, 5) CNT. Figure 1 shows the optimized geometries of the armchair (5, 5) CNTs with no defect and various defects such as a monovacancy, a substituted nickel atom, and a nickel adatom (obtained from the GGA calculations). Similar studies of defects in CNTs have been performed for various motivations [16, 17]. Our defective CNT structure with a substituted Ni atom in figure 1(c) has a bond length of ∼1.8 Å between the Ni atom and the surrounding carbon atoms in the CNT. (Note that all bond lengths hereafter are those obtained from the GGA calculations.) This is consistent with the previous reports [18, 19]. To find the stable position of the Ni adatom on the CNT, we considered many configurations and found that a corner of a hexagon in the CNT is most favorable, as shown in figure 1(d). On the other hand, the (8, 0) CNT has the most stable position of the Ni atom at a bridge in the axial direction [20].

Next, we investigate the binding strength of a Cu nanocluster (Cu_{13}) onto the CNT. Figure 2 shows the GGA-optimized structures of the model systems. The Cu_{13} clusters on the CNTs with no defect, a monovacancy, a substituted Ni atom, and a Ni adatom are shown in figures 2(a)–(d), respectively. We place the lowest-energy structure of Cu_{13} onto the defect-free or defective CNTs. For Cu_{13} on the defect-free CNT, the distance between $Cu_{13}$and the CNT is 2.16 Å, and the structure of Cu_{13} remains almost intact.

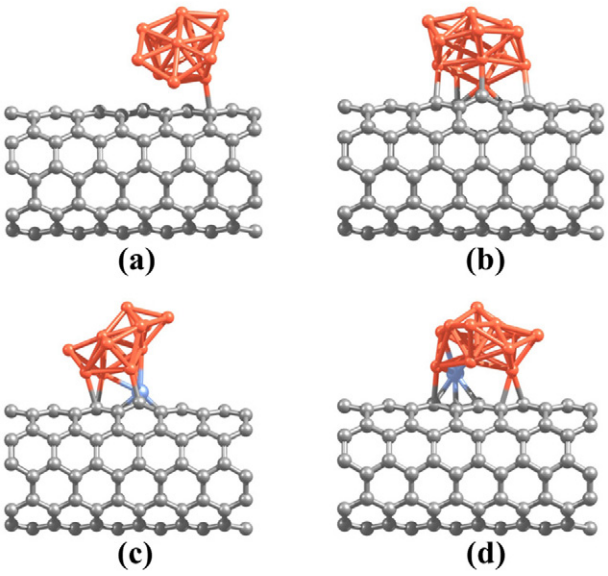

Figure 2. Optimized geometries of the adsorbed Cu_{13} clusters on the (5, 5) CNT with (a) no defect, and with defects such as (b) the monovacancy, (c) the substituted nickel atom, and (d) the nickel adatom.

The cases of the defective CNTs with the monovacancy, the substituted nickel atom, and the nickel adatom are depicted in Figures 2(b)–(d), respectively. We found that the binding energies of Cu_{13} are increased by the presence of defects on CNTs, as listed in table 1. In particular, the Ni adatom effectively contributed to the binding strength between Cu_{13} and the perfect CNT. In the case of Ni substitution, the Ni–Cu bond lengths are somewhat longer than 2.5 Å in GGA. For the Ni adatom, Ni–Cu bond lengths are in the range of 2.45–2.55 Å. The binding energies of the metal clusters on each case of CNTs were calculated as

$$E_{\mathrm{b}} = -[E_{\mathrm{tot}}(\mathrm{M_{13}/CNT}) - E_{\mathrm{tot}}(\mathrm{CNT}) - E_{\mathrm{tot}}(M_{13})],$$

where E_{tot} represents the total energy of the optimized geometry for each system and M_{13} indicates Al_{13} or Cu_{13}. The results of binding energy in both GGA and LDA are summarized in table 1. Although we did not consider all the possible geometries, the trend in table 1 is quite instructive: the binding of a Cu cluster onto a defect-free CNT is weak,

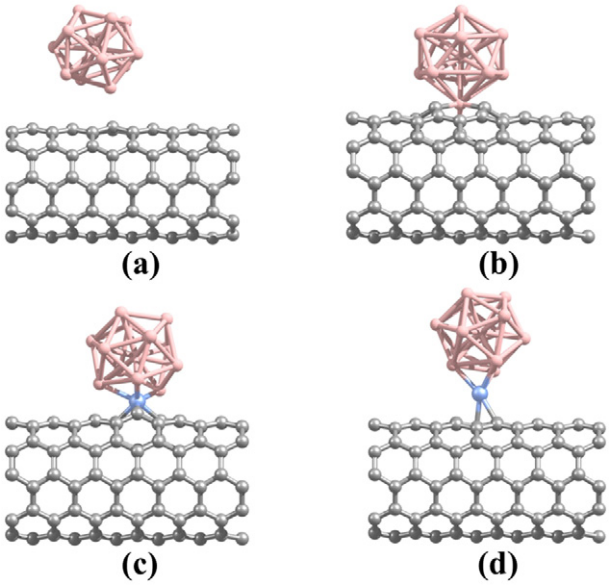

Figure 3. Optimized geometries of the adsorbed Al_{13} clusters on the (5, 5) CNT with (a) no defect, and with defects such as (b) monovacancy, (c) substituted nickel atom and (d) nickel adatom.

whereas their binding onto the defective CNT is quite strong. The strong binding character of Cu clusters onto the CNT with defects are consistent with the known chemical reactivities of defective CNTs. The defective CNTs have unsaturated dangling bonds of carbon sp^2 bonds, to which metal atoms are strongly bonded. The cases of the Ni adatom are more intriguing. The binding strength is much increased than the case of the CNT without defects. This suggests the potential of Ni adatom layers as a binder to clean CNTs. Previous calculations also showed the strong binding of a Ni atom onto a CNT [20]. Note that CNTs could be uniformly coated with layers of nickel atoms [21]. Thus, our calculations explain well the experiment by Lim *et al* [3] in that the presence of the nickel defects increases the binding strength between CNT and Cu clusters.

Now we turn to the case of Al_{13} with the same motivation as above. The GGA-optimized geometries for the Al_{13} cluster on the CNT with defects are shown in figures 3(a)–(d). Our *ab initio* study shows that the binding strength between Al_{13} and the defect-free CNT is weak. We previously reported that the binding energy of Al_{13} on the defect-free (5, 5) CNT is 0.04 eV (0.39 eV) in the GGA (LDA) calculations [22]. The shortest length between Al_{13} and the CNT is 2.43 Å. We calculated the models with defects such as monovacancy, nickel substitutional defect, and nickel adatom, as in the Cu_{13} case as discussed in previous paragraphs. We found that the binding strength is increased by the defects on CNTs (see table 1). The isolated structure of Al_{13} is almost preserved in the case of the defect-free CNT and the CNT with a monovacancy. For the nickel substitution, however, the structure of Al_{13} is deformed from its isolated geometry, and Ni–Al bond lengths are 2.36–2.47 Å. For the Ni adatom case, the slightly distorted Al_{13} cluster is attached to the Ni adatom which serves as a binder to the CNT, and Ni–Al bond lengths are 2.38–2.44 Å which is consistent with the increased binding strength shown in table 1. At this point, it is worthwhile noting the previous paper which reported the atomic adsorption of metals (Al and Cu) at SW defects in CNTs [9]. In that paper, the binding strength between the Al (or Cu) atom and the CNT slightly increases in the presence of the SW defect, whereas the binding energies of the metal nanoclusters increase substantially in the presence of all types of defects considered in our study. Thus, such a comparison may give some direct relevance of the previous calculations to ours in that defects in CNTs generally increase the binding energy of both metal atoms and nanoclusters.

To check the hybridization of the nickel atom impurity and the metal clusters, the projected densities of states (PDOSs) are plotted in figure 4. Figure 4(a) represents the PDOS of the substitutional nickel defect in the absence of the metal cluster. The d-orbital of the Ni atom is hybridized with the p-orbital of carbon atoms near the Fermi level and the available d-electrons of the Ni atom remain in the energy range between −3.0 and −2.0 eV. In the Ni adatom case, however, the available d-electron of the nickel atom is located in the energy range between −2.0 and 0.0 eV, as shown in figure 4(d). With binding to the metal cluster such as Cu_{13} and Al_{13}, the remaining d-electron of the nickel atom contributes to hybridization. The s- and p-orbitals of Cu do not contribute to the bonding with the nickel atom, whereas the d-orbitals are mainly involved in binding, as shown in figures 4(b) and (e). For the Al_{13} cluster, in contrast, p-orbitals of Al mainly affect hybridization between the metal cluster and the nickel atom, as shown in figures 4(c) and (f). This PDOS analysis demonstrates that the d-orbitals of Ni enhance the binding strength between the metal cluster and the CNT.

In addition to the binding properties, the magnetic properties of metal-coated CNTs have been attractive in terms of the one-dimensional magnet or the electrical interconnect. Thus, we also investigated magnetic properties of the CNTs with the monovacancy, the nickel substitution, and the nickel adatom. First, we calculated defective CNTs without clusters attached: the magnetic moments of CNTs with a monovacancy and a substituted nickel atom were found to be 1.45 μ_B and 0.67 μ_B, respectively. In contrast, the defect-free CNT with the Ni adatom has no magnetic moment, unlike the ferromagnetic bulk nickel. Note that the magnetic moment of a free-standing Al_{13} cluster is 0.98 μ_B, whereas Cu_{13} has a magnetic moment of 0.65 μ_B.

After attaching the metal clusters onto the defective CNT, nonzero magnetic moments were found for the Al cluster, but those of the Cu cluster had vanished. Al_{13} maintains its isolated structure on defective CNTs, but the shape of Cu_{13} is deformed from the original isolated structure, as shown in figures 2 and 3. This structural change in Cu_{13} originates from the strong covalent bonds with carbon atoms, and explains the disappearance of the magnetic moment of the Cu_{13}/CNT system. To investigate the effect of orientation of adsorbed clusters on the magnetic moment, we considered metal clusters with various adsorption orientations onto the CNT. As a result, we found the magnetic moment has negligible dependence on the orientation of adsorbed metal clusters onto the CNT. The magnetic moments of Al_{13} onto

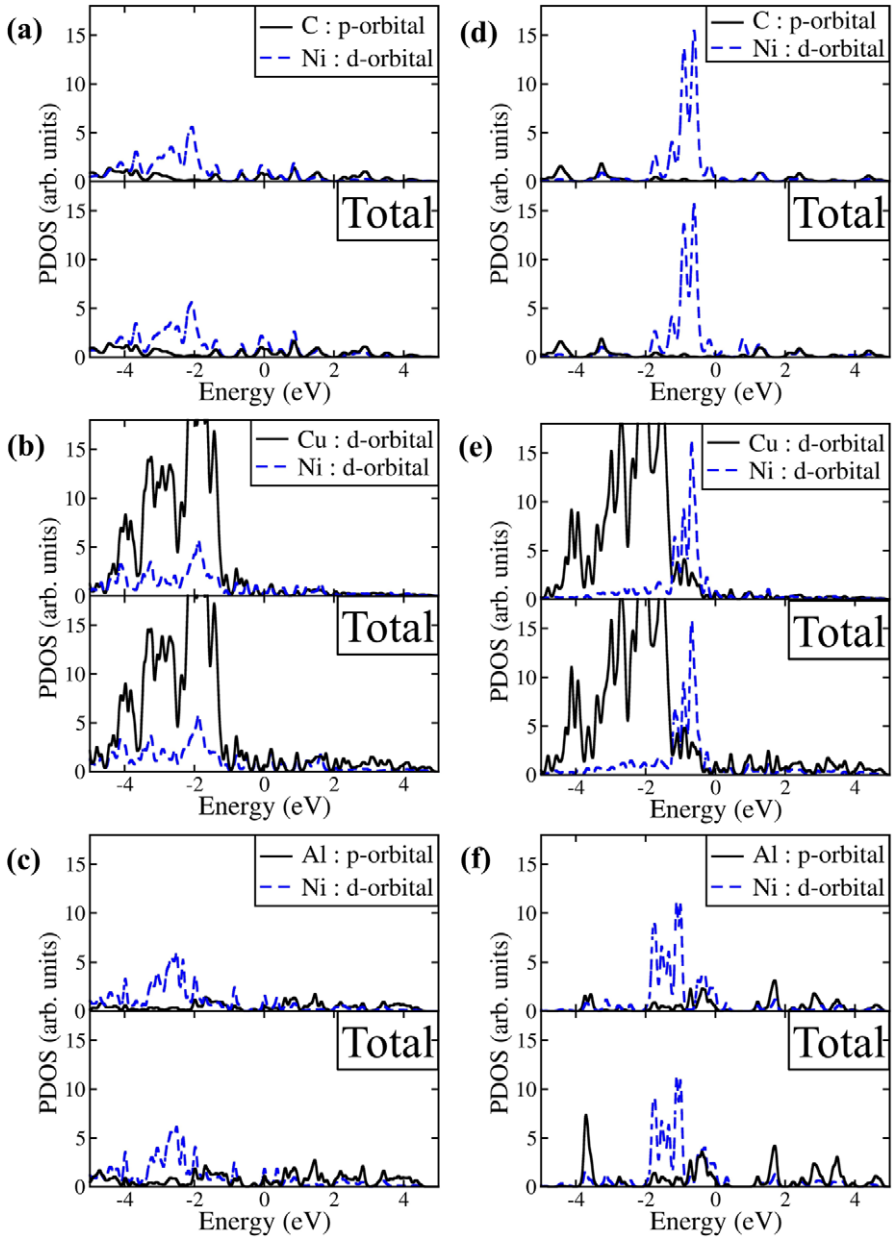

Figure 4. Projected density of states (PDOS) of (a) a substituted nickel atom, (b) a substituted nickel atom with a Cu_{13} cluster, (c) a substituted nickel atom with an Al_{13} cluster, (d) a nickel adatom, (e) a nickel adatom with a Cu_{13} cluster, and (f) a nickel adatom with an Al_{13} cluster, on the (5, 5) CNT. For comparison, the total DOS is plotted together. The blue dotted lines represent the PDOS of the Ni atom, and black solid lines show those of the carbon atom, the Cu_{13} cluster, or the Al_{13} cluster, respectively, in the parts of the figure. The Fermi level is set to be zero.

the defective CNT with the monovacancy and the substituted nickel atom are 0.96 and 0.79 μ_B, respectively. Since Al_{13} contains an odd number of aluminum atoms, it has unpaired electrons [23], contributing mainly to the magnetic moment of the Al_{13}/CNT system.

Figure 5 shows the spin DOSs for Al_{13} on the (5, 5) CNT with monovacancy and a nickel substitution atom, where we observe hybridization between orbitals of Al_{13} and the defective CNT. For both the monovacancy and nickel substituted cases, the main contribution of the magnetic moment comes from Al_{13}. In the latter case (see figure 5(b)), the defective CNT itself and the substituted nickel atom also contribute to the magnetic moment.

4. Conclusion

In summary, we have carried out *ab initio* DFT calculations to search for a reasonable way of enhancing binding strength of metal nanoclusters onto the CNTs. The effects of defects on CNT, such as the monovacancy, the Ni atom substitution, and the Ni adatom, were considered. We found that the weak binding strength of Cu and Al clusters onto CNTs can be substantially improved by the presence of those defects. In particular, the influence of the Ni adatom is the most outstanding. In conjunction with recent experiments of Ni coating, this suggests an efficient method for optimizing the metal–CNT complex nanostructures.

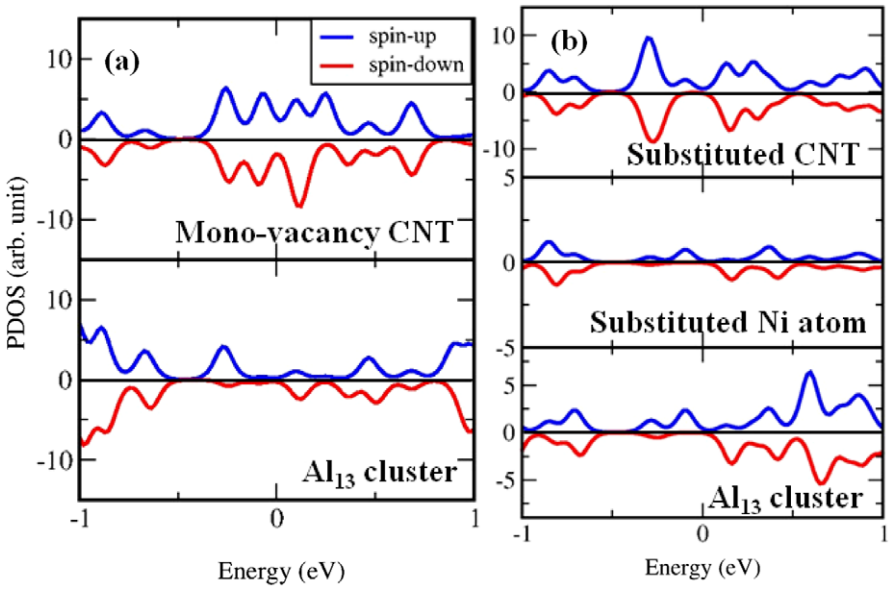

Figure 5. Spin DOSs for the Al_{13}/CNT system, where Al_{13} is adsorbed on the (5, 5) CNT with (a) a monovacancy and (b) a substituted nickel atom, respectively. The blue and red lines represent the up and down spins, respectively. Note that the scales of the vertical axes of (b) are different.

Acknowledgments

This research was supported by the Priority Research Center Program (2011-0018395), the Converging Research Center Program (2011K000620), through the National Research Foundation of Korea (NRF) funded by the Ministry of Education, Science, and Technology (MEST). Calculations were performed by using the supercomputing resources of KISTI. GK acknowledges the financial support by a grant from the MEST (Grant No. 2010-0007805). NP appreciates the support from the Hydrogen Energy R&D Center, a 21st Century Frontier R&D Program, funded by the Ministry of Science and Technology of Korea.

References

[1] Mamedov A A, Kotov N A, Prato M, Guldi D M, Wicksted J P and Hirsch A 2002 *Nature Mater.* **1** 190
[2] Thostenson E T, Ren Z and Chou T-W 2001 *Compos. Sci. Technol.* **61** 1899
[3] Lim B, Kim C-J, Kim B, Shim U, Oh S, Sung B-H, Choi J-H and Baik S 2006 *Nanotechnology* **17** 5759
[4] Cha S, Kim K, Arshad S N, Mo C and Hong S 2005 *Adv. Mater.* **17** 1377
[5] Xu L, Chen X, Pan W, Li W, Yang Z and Pu Y 2007 *Nanotechnology* **18** 435607
[6] Zhan G-D, Kuntz J D, Wan J and Mukhrjee A K 2003 *Nature Mater.* **2** 38
[7] Laha T, Agarwal A, Mckechnie T and Seal S 2004 *Mater. Sci. Eng.* A **381** 249
[8] Xu C L, Wei B Q, Ma R Z, Liang J, Ma X K and Wu D H 1999 *Carbon* **37** 855
[9] Meng F Y, Zhou L G, Shi S-Q and Yang R 2003 *Carbon* **41** 2023
[10] Ihm J, Zunger A and Cohen M L 1979 *J. Phys. C: Solid State Phys.* C **12** 4409
[11] Kohn W and Sham L J 1965 *Phys. Rev.* **140** A1133
[12] Kresse G and Furthmüller J 1996 *Phys. Rev.* B **54** 11169
[13] Kresse G and Furthmüller J 1996 *Comput. Mater. Sci.* **6** 15
[14] Perdew J P, Burke K and Ernzerhof M 1996 *Phys. Rev. Lett.* **77** 3865
[15] Ceperley D M and Alder B J 1980 *Phys. Rev. Lett.* **45** 566
[16] Okada S 2007 *Chem. Phys. Lett.* **447** 263
[17] Kim G, Jeong B W and Ihm J 2006 *Appl. Phys. Lett.* **88** 193107
[18] Andriotis A N, Menon M and Froudakis G 2000 *Phys. Rev. Lett.* **85** 3193
[19] Amara H, Roussel J-M, Bichara C, Gaspard J-P and Ducastelle F 2009 *Phys. Rev.* B **79** 014109
[20] Durgun E, Dag S, Bagci V M K, Yildirim T and Ciraci S 2003 *Phys. Rev.* B **67** 201401
[21] Zhang Y, Franklin N W, Chen R J and Dai H 2000 *Chem. Phys. Lett.* **331** 35
[22] Park N, Sung D, Lim S, Moon S and Hong S 2009 *Appl. Phys. Lett.* **94** 073105
[23] Rao B K and Jena P 1999 *J. Chem. Phys.* **111** 1890